REDUCING FLYOVER NOISE OF PROPELLER-DRIVEN AEROPLANES BY SUPERPOSITION OF PROPELLER- AND EXHAUST-NOISE

M. Kallergis

Institute for Design Aerodynamics
German Aerospace Research Establishment (DLR)
Braunschweig, Federal Republic of Germany

Abstract

The feasibility of attenuating propeller farfield noise is demonstrated by means of superimposing exhaust noise from the piston-engine with the very propeller noise so as to produce a destructive interference. Both the propeller noise and the engine exhaust noise signatures consist of a succession of periodic signals with "positive" and "negative" pressure parts. The problem is therefore the "adjustment" of the propeller sound signal so that it is precisely in anti-phase with the exhaust noise signal. A potentially promising way to achieve such an objective lies in the adjustment of the relative circumferential position of the propeller blades to the crank shaft such that - at any particular observer position on the ground - "sound" and "anti-sound" would combine to produce a reduced level.

To substantiate this concept a theoretical and experimental study was initiated. In order to support the theoretical findings, flight tests with a Cessna T 207 aircraft were executed. A special flange was inserted between the propeller and the drive shaft. The flange could be rotated in steps, thus shifting the phase of the sound waves as radiated from the propeller with respect to those of the engine exhaust. Acoustic measurements with a wing-mounted microphone indicated the feasability of the concept in the near-field of the aircraft, where A-weighted overall level differences between 3 and 4 dB were observed. Flyover noise tests on the farfield effects using a microphone on the ground indicated a noise reduction potential from 4 to 6 dB between particularly good and bad relative propeller blade positions.

INTRODUCTION

The concept of active sound attenuation as first published in the early thirties by Lueg |1| used an "artificially" produced sound to counteract unwanted noise. The reactive suppression in the near-field of a primary source has been particularly investigated by Nelson et al. |2, 3|. The attenuation of a sound field radiated by a point source by using an adjacently placed monopole source as a simple example of the active control of sound has been discussed more recently by Ffowcs Williams |4|. A practical use of this concept was demonstrated by Chaplin |5| who succeeded in reducing the periodic sound as radiated by the exhaust of an internal combustion piston engine. A proposal to reduce the noise of overflying propeller driven aeroplanes using anti-noise loudspeakers or sirens installed under the wings was made by Bschorr in 1973 |6|. Most of these concepts however pertain to stationary problems where the source does not move with respect to the receiver.

Active noise attenuation by destructive interference of the sound radiation from a primary and from a secondary acoustic source has thus long been recognized as a promising means to reduce the noise especially of low-frequency sources. To reduce the noise of a piston-engine-powered propeller aeroplane one might consider the propeller to represent a primary source whose radiative field is to be appropriately superimposed with the sound field of the engine exhaust as the secondary source.

Within a theoretical and experimental study a method was developed and its feasability demonstrated to attenuate the rotational (harmonic) noise from overflying aeroplanes by adjusting the propeller noise in anti-phase to engine noise. A reduced overall acoustic power output can be achieved by appropriately arranging the secondary source (piston-engine), whose strength is allowed to differ in magnitude from the primary source (propeller). It is important to point out that, when a noise source is moving or another source is added, then the result is a complex acoustic radiation pattern. In most cases this pattern is distinctly different from that of a source at rest in a free field. Static acoustic measurements made for the purpose of characterising the source behaviour or of understanding the very noise generating mechanisms must accordingly be corrected for motion and the effect of interference. The need to make such corrections and the accurate prediction of noise of moving individual sources (or of systems of sources) from first principles requires a thorough quantitative understanding of these effects. It is important to realize that kinematic and dynamic effects of forward motion and interference of sound of the sources play a significant role in the measurement and prediction of noise from aircraft.

In this paper some theoretical results on the influence of the proximity of sources and of their motion on the radiation from acoustic monopole and dipole sources are presented and experimental findings are reported on propeller and exhaust noise interference effects during flight. Parts of this work are based on earlier studies by the author and one of his collaborators (7, 8, 9, 10).

THEORETICAL CONSIDERATIONS

Calculation of the Intensity Radiation Pattern

The sound field of a propeller driven aeroplane may be derived by superimposing propeller noise and engine exhaust noise. The sources of both these harmonic noises produce again a harmonic noise pattern with a certain amount of higher frequency components. In order to use the sound sources in an efficient manner for purposes of destructive interference, pressure amplitudes of equal magnitude and good phase matching of the sources are an important prerequisite.

Following Gutin's classical theory for propeller noise (steady blade forces in a rotating reference frame) and using an approximation by Goldstein |11| in which directivity and phase information are preserved, and furthermore assuming a monopole for the engine exhaust orifice, the normalized intensity in the far-field may be expressed as:

$$I' = F_n^2(\sin\vartheta)^{2nB}(\cos\vartheta+c_f)^2 + \frac{\hat{\Phi}^2_R}{4\pi} + \frac{\hat{\Phi}_R}{\sqrt{\pi}} F_n(\sin\vartheta)^{nB}(\cos\vartheta+c_f)\cos\Theta \qquad (1)$$

$$\Theta = [2\pi(e'\cos(\varphi-\varphi_A)\sin\vartheta + a'\cos\vartheta) - nB(\varphi-\Delta\varphi-\tfrac{\pi}{2})]$$

(in this case no individual phase shifting of the higher harmonics of the engine exhaust noise is made). Here, n and B are the higher harmonic order and the number of blades, respectively, $\phi_R = \phi_A/\phi_P$ is the ratio of the engine exhaust and propeller velocity potentials and c_f is a factor which is usually somewhat less than unity ($c_f \approx 0,9$), thus not significantly influencing the directivity pattern. e' and a' are the distances of the engine exhaust orifice from the propeller axis and from the plane of rotation, respectively, divided by wave-length. The normalizing function F_n and the geometric data can be taken from

$$F_n = \left[\frac{1}{2\pi\int_0^\pi(\sin\vartheta)^{2nB+1}(\cos\vartheta+c_f)^2 d\vartheta}\right]^{1/2}$$

and from Fig 1.

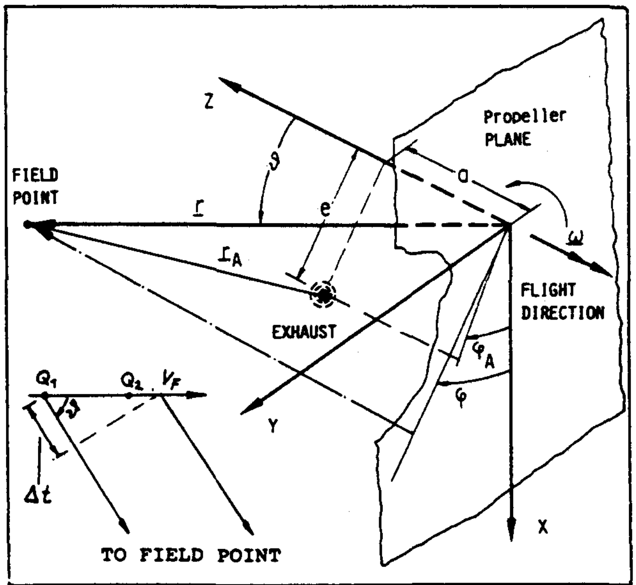

Fig. 1 Coordinates of Propeller and Exhaust Relative Positions for establishing an Acoustic Model; (Sources in Motion)

The intensity I was normalized with

$$I' = \frac{I}{\rho K_{nB} nB\ \omega\hat{\Phi}_p^2/2r^2}$$

ρ being the density, K_{nB} the wave number related to the nB order of harmonics and ω the radian frequency of the sources, respectively. For simplicity the intensities of the propeller and engine exhaust sound were assumed to be equal. As in the case of a source near a wall (image source) this superposition of the sound fields causes a complicated intensity radiation pattern showing a number of lobes.

The number of lobes in the propeller plane depends on the term $nB\varphi$ in eq. (1). In case of a 3-blade-propeller the intensity radiation pattern consists of e.g. three maxima for the first and of fifteen maxima for the fifth harmonic (Fig. 2). The lobes differ in shape since the angles between the maxima are different. The orientation of the interference pattern in the propeller plane with regard to a symmetric axis depends on the

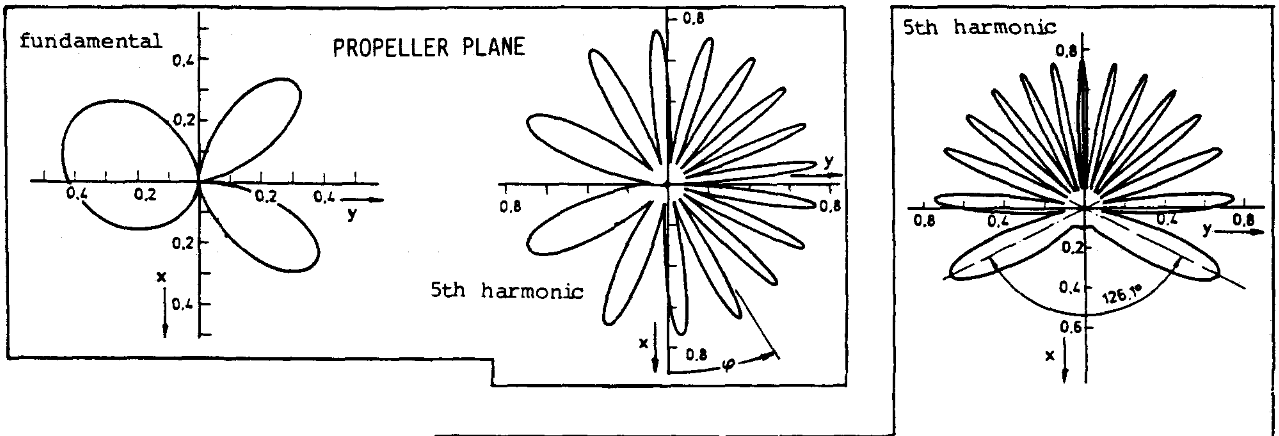

Fig. 2 Intensity Radiation Patterns of a Propeller Exhaust System from Common Aeroplanes

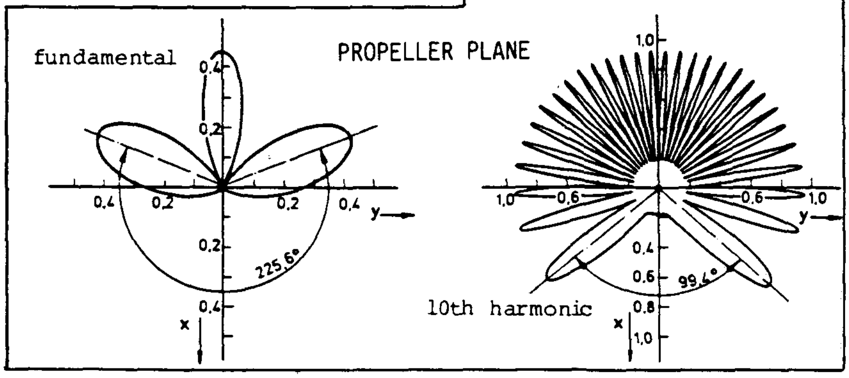

Fig. 3 Intensity Radiation Patterns of a Propeller-Exhaust System after an Optimisation of the Source Relative Positions

phase difference between propeller sound and exhaust noise. It may vary as a result of an azimuthal displacement of the propeller relative to the crank shaft. An orientation of the narrowly spaced lobes towards the ground is disadvantageous and should be avoided (as illustrated in Fig. 3/right half on the 5th harmonic pattern).

Local Interferences

According to classical calculation examples dealing with elementary sources it is desirable to replace the cosine argument θ in the third summation part of eq. (1) by a suitable value of $\Delta\varphi$ in the argument to give a value of $\cos\theta = -1$. This would result in a reduction of the intensity maximum

$$\Delta I'_{max} = -\frac{Fn}{\sqrt{\pi}}\hat{\Phi}_R(\sin\vartheta)^{nB}(\cos\vartheta+c_f)$$

To reduce the sound radiation towards the ground it is even more important to specifically adjust the interference pattern as described in the following: The maximum intensity lobes forming the largest aperture angle $\Delta\varphi_{max}$ can be positioned symmetrically to the vertical axis. This causes a 'zone-of-silence'-aperture underneath the aeroplane. This maximum angle can be opened up still further by certain additional steps (to be explained further down). The propagation distances for the sound waves which are oriented in the direction of these maxima, are now much larger before they hit the ground. The sound pressure level difference for the spreading reduction compared with a vertical radiation is $\Delta L_p = 20 \log (\cos \varphi)$ (see Fig.2).

The nB maxima in eq. (1) appear at the angles $\varphi^{(m)}_{max}$ on the circumference, when the argument of the cosine term is an integer multiple of 2π.

$$2\pi[e'\cos(\varphi^{(m)}_{max}-\varphi_A)\sin\vartheta+a'\cos\vartheta]-nB(\varphi^{(m)}_{max}-\Delta\varphi-\frac{\pi}{2}) = 2\pi m \qquad (2)$$

where m is a natural number which sequentially designates the successive maxima.

The *dimensionless distances e' and a'* are now expressed as $e' = efnB/c = e_o nB$ and $a' = afnB/c = a_o nB$. Now eq. (2) may be rewritten in an implicite form

$$\varphi^{(m)}_{max} = 2\pi[e_o\cos(\varphi^{(m)}_{max}-\varphi_A)\sin\vartheta + a_o\cos\vartheta - \frac{m}{nB} + \frac{1}{4}] + \Delta\varphi \qquad (3)$$

The term $2\pi\, a_o\cos\vartheta$ causes a rotation of the interference pattern during the fly-over. If this rotation is to be avoided, with regard to the closer spaced maxima of the higher order harmonics, the distance a_o between engine exhaust and propeller plane must be minimized. The term $2\pi e_o \cos(\varphi^{(m)}_{max} - \varphi_A) \sin\vartheta$ describes a deformation of the circumferential distribution of the maximum values from the interference pattern. It is obvious that the circular position φ_A of the engine exhaust has separated the entire lobed pattern into two semi-circles. One of them - included between the angles $-180° + \varphi_A$ and φ_A - contains growing angles, the other semi-circle contains the contractions of the angles between the lobes. In order to put the particular pattern (with increases of angles) towards the ground, the attitude of the exhaust should therefore assume an angle of $\varphi_A = 90°$. Furthermore, to achieve a symmetrical adjustment of the largest aperture angle $\Delta\varphi^{(m)}_{max}$ between two maxima during the flyover a value of

$$\Delta\varphi^{(m)}_{max} = \varphi^{(m)}_{max} - \varphi^{(m+1)}_{max}$$

using eq. (3) is formed, i.e.

$$\Delta\varphi^{(m)}_{max} = 2\pi \left[e_o [\cos(\varphi^{(m)}_{max} - \varphi_A) - \cos(\varphi^{(m+1)}_{max} - \varphi_A)] \sin\vartheta + \frac{1}{nB} \right] \tag{4}$$

For a distance between engine exhaust and axis of rotation $e_o = 0$, eq. (4) in the overflight position ($\sin\vartheta = 1$) yields an equidistant distribution of the maxima $\Delta\varphi^{(m)}_{max} = 2\pi/nB$. With respect to an increase of the angle between two maximum lobes $\Delta\varphi^{(m)}_{max}$, it is more advantageous to optimise the distance e_o of the exhaust to the axis to ensure an increase of this angle instead of setting $e_o = 0$.

After optimisation of e_o, the maximum achievable angles $\Delta\varphi^{(m)}_{max}$ for a certain rotational speed can be determined. An exact adjustment of those $\Delta\varphi^{(m)}_{max}$ for all phases of both sources which are symmetrical to the vertical axis can be carried out by "tuning" the phase difference $\Delta\varphi$ on the propeller shaft.

With some precautions, such as

- eliminating a_o to avoid changes of the signal distances to the receiver on ground during flight,
- setting exhaust orientation $\varphi_A = 90°$ to direct the particular best suited angle with increased angles between the lobes towards the ground, and
- adjusting the phase difference at a value of $\Delta\varphi = -30°$ (which means that angle spreadings of the interference patterns are symmetrical toward the ground)

the following very promising results may be achieved.

Example:

Assume the following conditions:

e = 1,25 m;
a = 0 m;
φ_A = 90°;
$\Delta\varphi$ = -30°; and
a rotational speed range from 2500 to 2600 RPM.

Although these conditions may not be actually realized in practice, beneficial spreading angles $\Delta\varphi^{(m)}_{max}$ as well as substantial noise level reductions ΔLp are computed. For the

fundamental: $\Delta\varphi_{max}$ = 225,6°; $\Delta Lp \hat{=}$ no components to the ground

5th harmonic: $\Delta\varphi_{max}$ = 126°; ΔLp=-6,9 dB

10th harmonic: $\Delta\varphi_{max}$ = 99,4°; ΔLp=-3,8 dB

As shown in this example and in Fig. 3, slight changes of the position of the exhaust and the adjustment of phase differences result in large spreadings of the angles between the lobes with considerable reductions of the noise radiation towards the ground.

EXPERIMENTAL ASPECTS

Test Aeroplane

Near-field noise experiments were conducted on a Cessna T 207 airplane, equipped with a Teledyne Continental six-cylinder, four-stroke turbo-charged piston engine of 212 kW rated power and a McCauley three-blade variable-pitch propeller of 2,03 m diameter (Fig. 4). The aircraft was typically flown in level flight at constant flight speed of 60 m/s. Additional near-field noise experiments were perfored with a Hartzell two-

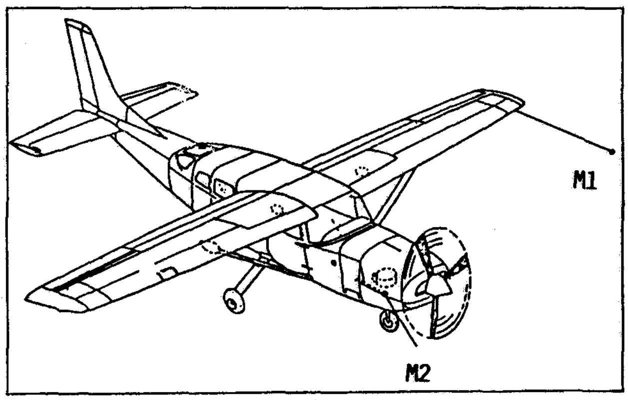

Fig. 4 Test Aeroplane Cessna T 207 with Wing-mounted and Engine Exhaust Positioned Microphones

blade variable-pitch propeller of 2,03 m diameter.

The aircraft was equipped with a wing-mounted microphone M1 for fixed-position near-field noise studies. Measurements with such airplane-attached microphones are inherently free from ground-reflections and cross-wind effects, which necessarily occur in flyover ground-based measuremnts. Moreover, there is no Doppler-effect, allowing the gathering of accurate base-line data. In contrast to wind tunnel tests on isolated propellers, however, the very propeller noise is "contaminated" with engine noise contributions. Therefore, the aeroplane was equipped with a microphone M2 close to the engine-exhaust orifice to allow an identification and quantification of the engine noise.

Engine Noise Characteristics

As shown in Fig. 5, top, the signature of the four-stroke engine at constant rotational speed and torque exhibits a succession of signals of characteristic shape and amplitude. Each signal corresponds to one working cycle of a piston. The individual engine pressure signals consist of "positive" and "negative" components, as evident from the pressure-time histories from the six-cylinder engine shown in the Figure. Each engine pressure signal has its own characteristics, affected by the combustion processes, and the propagation within the cylinder outlets and in the exhaust system. The very propeller wake may to some extent also affect the exhaust noise, its effect however being minimal. Considering a longer sequence of 3.5 working cycles (Fig. 5, bottom), one may observe that each of the six individually formed signals belonging to any particular cycle are repeated in a time span corresponding to two revolutions (≙ one firing cycle of the four-stroke engine). This becomes more obvious still, if signals with identical numbers are considered. The distance in time between these signals corresponds to $t_A = 2 \cdot 60/n = 46$ ms for a rotational speed of $n = 2600$ RPM, related to a sequential time between two firings $t_z = 2 \cdot 60/z \cdot n = 7{,}7$ ms, where Z is the number of cylinders. Signals of identical number show an identical shape.

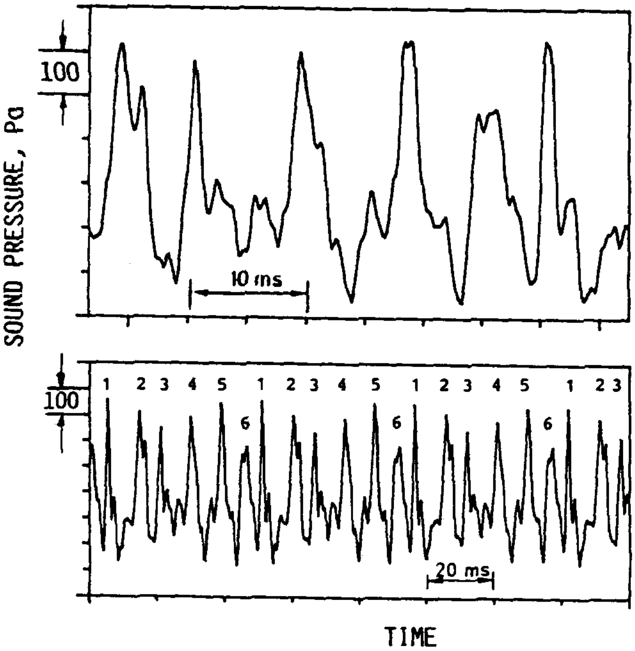

Fig. 5 Engine Exhaust Sound Pressure Signatures

In contrast to the propeller noise signals, the time span from one signal to the next is not the same. This is a consequence of the particular shape of the exhaust system of the turbo-charged engine (Fig. 6). The exhaust system of the same engine without turbo-charger consists however of two simple pipes (Fig. 7).

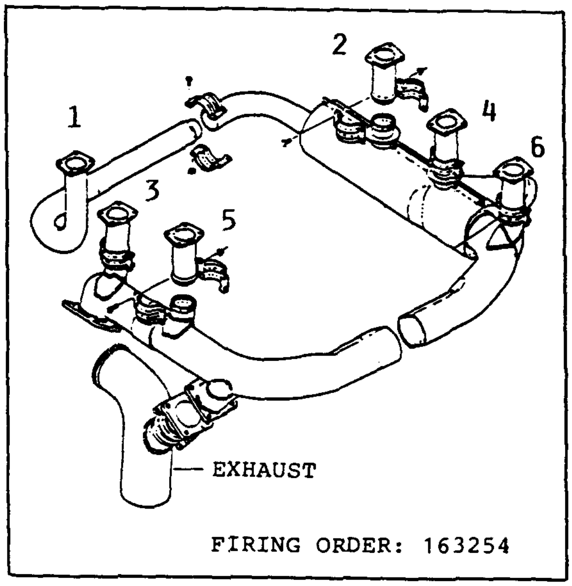

Fig. 6 Exhaust System of the Continental Turbo-charged Engine

Propeller Noise Characteristics

As shown in Fig. 8, at blade helical tip-Mach-numbers MH* greater than 0.7 the pressure time history signal of a rotating propeller consists of a sequence of distinct impulses. They possess "posi-

---

* $MH = \sqrt{v^2 + (\pi D\, n/60)^2}\,/c$ with v = true airspeed of the aeroplane in m/s, D = propeller diameter in m, n = propeller speed in RPM and c = speed of the sound in m/s

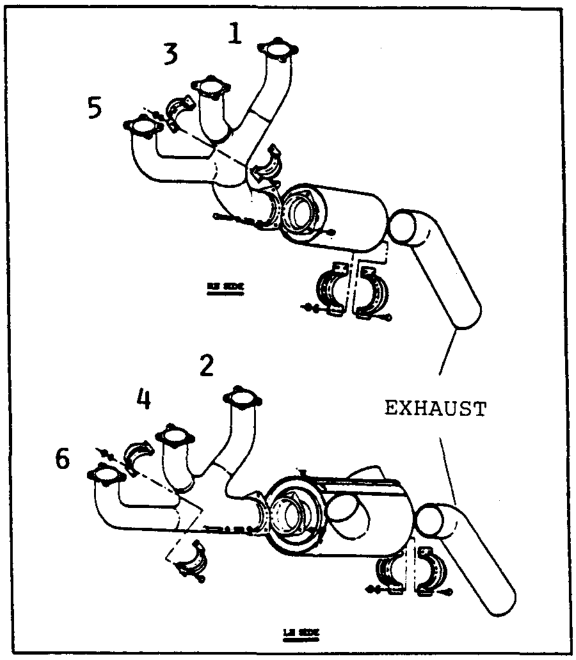

Fig. 7 Exhaust System of the Continental Engine without Turbo-charger

tive" and "negative" parts, each one "impulse" corresponding to one each blade for one propeller revolution. This Figure shows data for a constant MH = 0,83 for microphone position M1. M1 is located 4 m from the propeller axis to the leeward side, 1 m aft of the propeller-plane. At a speed of 60 m/s this microphone measures noise signals that were propagating in the plane of rotation. It is obvious, that the positive components exhibit an approximate saw-tooth shape. In contrast,

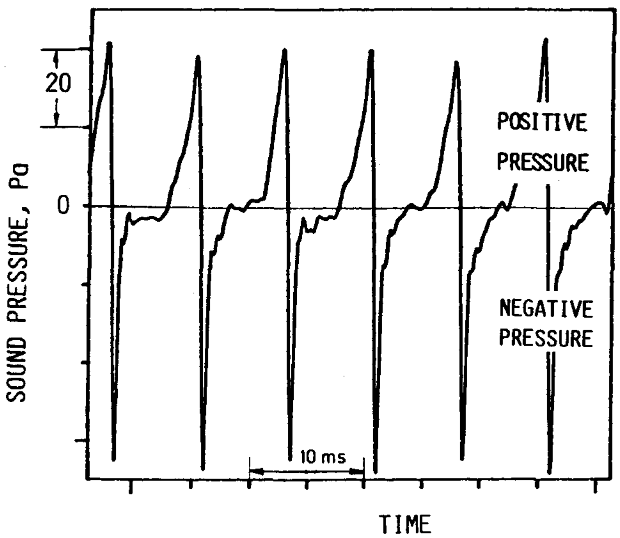

Fig. 8 Propeller Noise Signature at Constant Helical Blade Tip Mach Number

at the normal speed of the propeller, a relatively narrow peak pressure pulse is formed on the negative pressure side.

At moderate tip Mach numbers, rotating blades produce both monopole (thickness) and dipole (thrust and torque related loading) type noise. The sound field from rotating blades is periodically in time with 60/B•n, where B is the number of blades and n is the shaft speed. At a constant rotational speed the time span between two signals is constant and can be exactly calculated.

Narrow-band analysis of signal sequences, as represented in Fig. 8, shows that the distinct negative pressure part of the signals are responsible for a spectrum with substantial higher frequency content, which largely determine the A-weighted level. A "narrowing" of the negative pressure peaks thus causes the A-weighted level to increase.

Superposition of Signals in the Time Domain

For the typical aeroplanes the phase angle between propeller sound and engine noise is in no way optimized: the time of the emission of the acoustic sound waves from the propeller and from the engine exhaust are not adjusted to result in minimum sound radiation (and often, after an overhaul, the propeller is put back on the crank shaft in a different circumferential position). In practice, the signal sequences of engine and propeller are propagating with a fixed time delay just as chance would have it. Moreover, in the process of measuring flyover noise of two sources separated by a certain distance, the ensuing sound waves are continuously shifted with respect to a stationary observer on the ground. It is of interest, therefore, to determine in advance, and prior to any actual flyover noise testing, how the combined signal changes after a propeller was adjusted in different circumferential positions.

A computer-simulation was carried out by shifting two series of propeller noise signals and engine exhaust noise signals in small incremental steps and adding their pressures. Fig. 9 shows a typical result with two series of signals as measured on the test aeroplane Cessna T 207 in flight. The signals of the two concurrent sound sources are plotted on the top of the Figure, the propeller noise (left) and the exhaust noise of the engine (right) as measured at microphone M1 position (see Fig. 4).

In this procedure the exhaust signal, originally measured at position M2 (see Fig. 4) was attenuated to correspond to the sound pressures at microphone position M1.

Inspecting the signals obtained in the anti-phase superposition, it is obvious that not each individual pattern is reduced at the same rate. As the computer

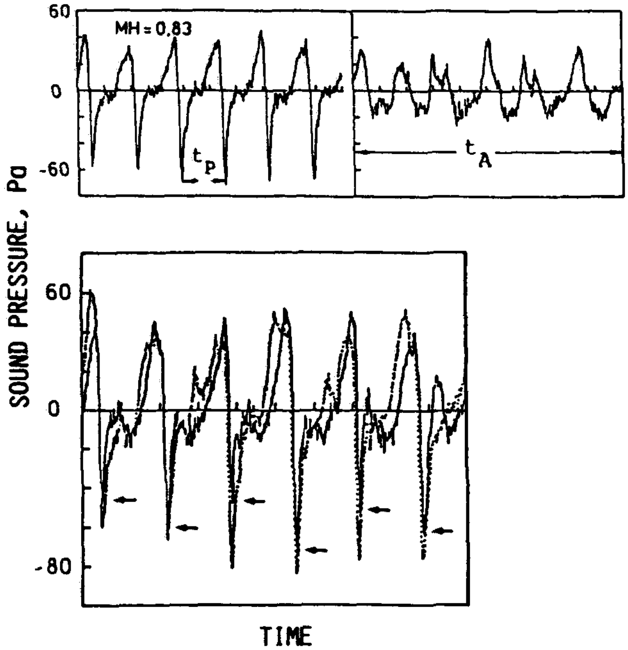

Fig. 9 Top: Noise Signatures from Propeller (left) and from Engine Exhaust (right)
Bottom: Superimposed Pattern In-Phase (dotted) and in Anti-Phase (⟵ mark ends of shorted amplitudes)

simulation was carried out with measured values, this might be due to the form of the (ring-shaped) collecting-pipe of the exhaust (see Fig. 6) of the turbo-charged engine. Although the distribution of the ignition points over the working cycle is symmetrically, the resulting ignition pressures are not equally spaced in time. This is however an important requirement for matching exactly all propeller and exhaust patterns. A thorough matching would be possible, if an exhaust pipe was used like that of Cessna 207 A, where three cylinder outlets on each side of the engine are reduced to one common exhaust pipe (see Fig. 7). Corresponding observations have already been made under actual measuring conditions, as reported in the Section below.

Combinations of Propeller-Blade and Engine-Cylinder Numbers

As mentioned before it is mandatory that a sound pressure signal from one cylinder coincides with a sound signal emitted by one propeller blade. This is the case, for example, with a 4-cylinder four-stroke engine in connection with a two-blade propeller, but also with a 4-cylinder two-stroke engine in connection with a four-blade propeller. In contrast, with a 6-cylinder four-stroke engine having a two-blade propeller, only one blade sound signal is available for three cylinder sound signals. There would still be a small noise reduction.

In general, the number of the propeller-blades B and the number of the cylinder ignitions per revolution of the propeller shaft C must yield an integer ratio. A ratio of B/C = 1 is to be preferred, where maximum noise reduction would be achieved. Table 1 presents the ratios B/C of the number of the propeller-blade noise pressure signals to the number of the engine cylinder noise pressure signals per revolution of the propeller for different engine/propeller combinations with and without gears. A noise reduction for each blade pressure signal occurs when the magnitude of the ratio B/C is equal to 1. Other ratios - smaller or larger than 1 - would result in a less good reduction. Again, B/C = 1 would provide an optimum result. For attenuation of half of the blade pressure signals the characteristic value B/C = 2 gives an average result. The characteristic value B/C = 1/2 indicates that, for attenuating one blade pressure signal, two cylinder pressure signals are available in correct anti phase.

Table 1. Combinations of Propeller and Exhaust Sound Pressure Impulses for Typical Aeroplanes to result in Characteristic Values B/C;

B being the number of blade sound pressure impulses per revolution of propeller shaft;

C being the number of cylinder sound pressure impulses per revolution of propeller shaft

	4-stroke		2-stroke						
drive	direct		direct			reduction 2:1			
cyl.	4	6	2	3	4	1	2	3	4
B \ C	2	3	2	3	4	2	4	6	8
2	1	-	1	-	1/2	1	1/2	-	-
3	-	1	-	1	-	-	-	1/2	-
4	2	-	2	-	1	2	1	-	1/2

The sequential times between two signals of the propeller and engine sound-field may be estimated from the left or right hand parts of the following equations; if the signals have to be matched to achieve attenuation then the two equations must be satisfied:

$1/B \cdot n_p = 2/Z \cdot n_M$ for four-stroke engines
$1/B \cdot n_p = 1/Z \cdot n_M$ for two-stroke engines

with B being the number of blades, Z the number of cylinders, n_p and n_M the RPMs of the propeller and engine, respectively.

If a reduction gear of an-even numbered-ratio $r = n_M/n_p$ is used then n_M must be substituted by $n_M = r \cdot n_p$ in the equations.

FLIGHT TESTS

In-Flight Measurements

Phase Shifting Device

The purpose of the test flights has been to show whether positive and negative parts from the propeller sound pressure interfere with those of reverse sign from the engine exhaust. In this case similar results to those achieved from the computer simulation are to be expected. These in-flight experiments were not specifically directed towards generating global reductions of sound in space but rather to test the occurence of a directional attenuation underneath the aeroplane. Therefore, it was considered primarily important to investigate the interference effects - such as attenuations or reinforcements - in the direction of the wing tip microphone for an optimisation of the superposition of sound pressures. Fig. 10 schematically illustrates the overlapping sound fields close to the aeroplane and the microphone

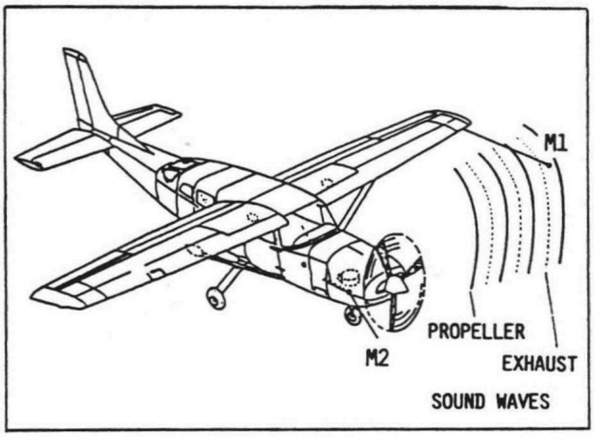

Fig. 10 Sound Fields due to Propeller and Engine-Exhaust Close to the Test Aeroplane

positions at the tip of the wing as well as close to the engine exhaust.

To carry out experiments on active attenuation of sound fields near an aeroplane the aircraft was now equipped with a special flange inserted between crankshaft and propeller as shown at the top of Fig. 11. This special flange consists of two discs, each of them being mounted to the propeller and the drive shaft by bolts. To shift the phase of the sound waves, as radiated from the propeller in relation to those from the engine exhaust, the two discs could be rotated stepwise against each other (see bottom of Fig. 11).

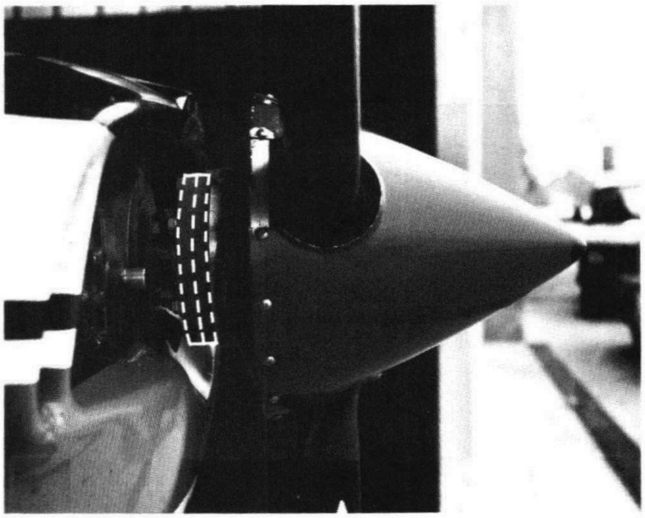

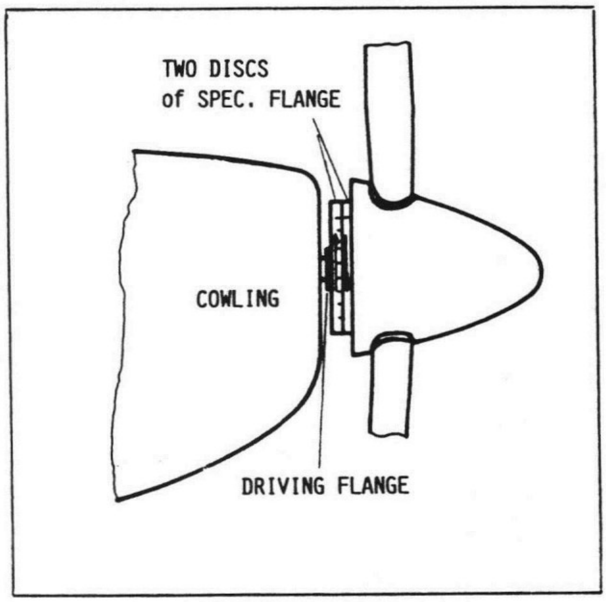

Fig. 11 Special Flange on Test Aeroplane

The change of the two discs of the flange for the subsequent adjustment could then be done on the ground with the engine stopped. The smallest angle between both discs is 7,5°. This corresponds to a shift of the sound fields by 0.48 ms at a propeller rotational speed of 2600 RPM. Fig. 12 shows the changes of the phase angle between the crank shaft and the propeller. Those changes accomplished an overlapping "dial-sector" between two blades amounting to 120°. Thus, 16 posi-

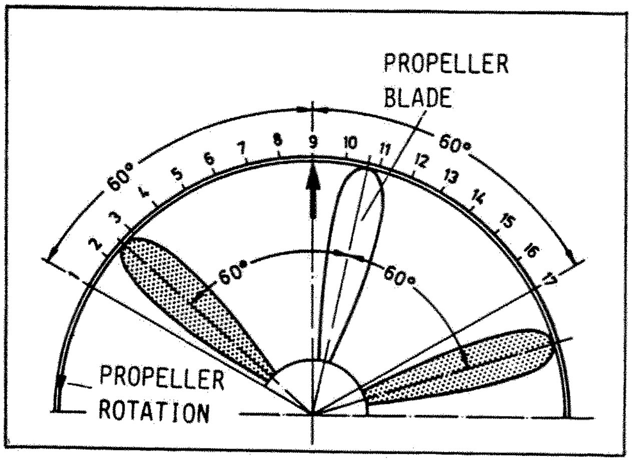

Fig. 12 Phase-Shift Adjustment between Crank Shaft and Propeller

tions, each of 7,5°, had to be adjusted. It might be helpful to note some important time intervals refering to an engine speed of n = 2600 RPM:

- length of the working cycle of the engine

$$t_A = \frac{2 \cdot 60}{n} = 46 \text{ ms}$$

- time for one shaft revolution

$$t_W = \frac{60}{n} = 23 \text{ ms}$$

- time between two blade sound patterns

$$t_P = \frac{60}{B \cdot n} = 7{,}7 \text{ ms}$$

- time between two cylinder sound patterns

$$t_Z = \frac{2 \cdot 60}{Z \cdot n} = 7{,}7 \text{ ms}$$

- lower limit of angular change corresponding to a time shift

$$t = \frac{60}{16 \cdot B \cdot n} = 0{,}48 \text{ ms}$$

Experimental Results

Fig. 13 shows the overall sound pressure patterns as measured at microphone M1 and changing the relative positions between the two discs. These changes demonstrate the effect of superposition of sound pressures from a specified blade and one specified piston at different phase shifts. On each trace, the sound pressure pattern from the engine exhaust (broken

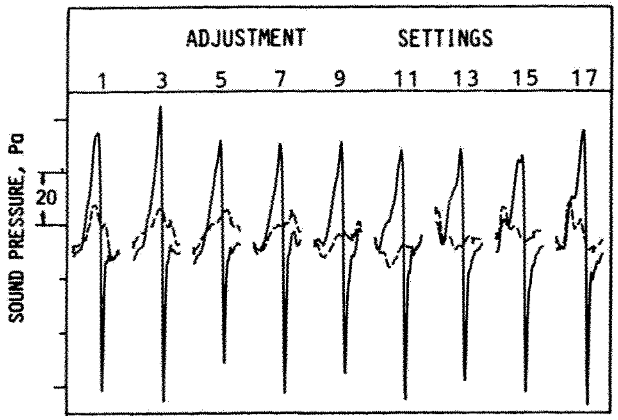

Fig. 13 Effect of Phase Shift on Overall Sound Pressure Patterns

lines) is indicated. Changing the adjustment settings - from No. 1 to No. 17 - the exhaust trace now changes its position relative to the overall pressure patterns. In this way the effect of individual phase shifts can be followed. Deformations of the overall patterns - like a "thickening" with positions 15 and 17, amplifications with positions 3 and 17, attenuations with positions 5, 9 and 13 - are produced by different phase shifts between propeller and exhaust sound waves.

To achieve attenuations of the sound pressure levels the relative phase shifts between the sound pressures should be like those with positions 5, 9 and 13, of course. Positions like 15, 17 and 3 yield unwantedly higher levels. To illustrate the potential inherent in such superpositions two arrangements of measured pressures are shown in Fig. 14. Here, on top two measured propeller pressure patterns of virtual identical shape (———) after superposition with engine exhaust patterns (— — —) produce quite different peak-to-peak amplitudes and shapes (bottom of the Figure): in-phase left trace and out of phase right trace. The pronounced negative pressure part of the pattern (left) - which predominantly affects the tonal content of the spectrum - is attenuated (right).

Flyover Measurements

Subsequent to the near-field noise measurement on the test aeroplane itself, flyover measurements were executed to check whether observed near-field effects in the noise field would extend to the ground.

As mentioned before, the pressure pulses of the turbo-charged engine of the test aeroplane are not equally spaced in time during any given working cycle. If an exact destructive interference of all sound impulses from the propeller is to be achieved, then the requirement of

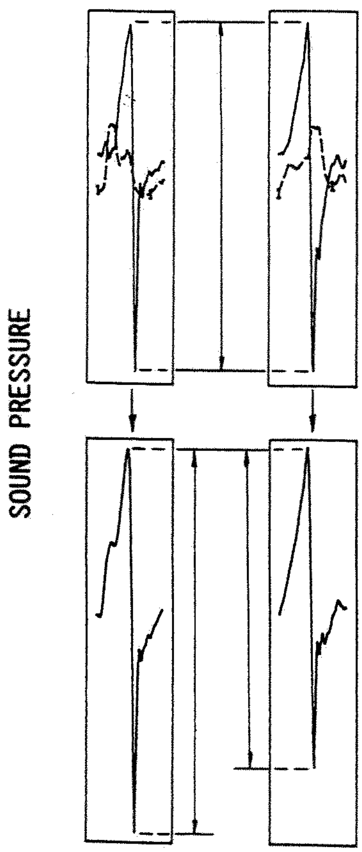

Fig. 14 Top: Superimposed Propeller- and Exhaust-Sound Pressure Pattern In-Phase (left), Out-of-Phase (right)
Bottom: Overall Sound Pressure Pattern

equal distances is to be strictly observed. Therefore, measurements as presented in the following yield interferences of single impulses only as observed during the in-flight tests.

Significant sound pressure level attenuations on the ground require precise destructive superpositions of the sound waves over a sufficiently long time duration of a flyover. As shown previously, in order to achieve this effect, the distance between engine exhaust and propeller plane must be as small as possible. This minimum distance is 0.7 m for the test aeroplane, in which case alternating pressure attenuations and reinforcements would result in a rotation of the interference pattern.

More precisely: a relative change of the time difference Δt between two distinct impulses from propeller and engine exhaust noise as measured on the ground does indeed occur (Fig. 15). This time difference now consists of two parts, as can be shown by a model (see Fig. 1) using two monopole sources in motion of the same frequency. The distance between the two sources is assumed to be a, their constant velocity V_F. If source Q_2 is emmiting a time $\Delta\tau_e$ later than source Q_1 , then the difference of the sound rays to a receiver on the ground is
$S_2 - S_1 = a \cos\vartheta + V_F \Delta\tau_e \cos\vartheta$. From this equation the difference Δt can be extracted,
$\Delta t = \Delta\tau_e (1 - M_F \cos\vartheta) - a \cos\vartheta / c$, where M_F is the flight Mach-number, c the velocity of the sound and ϑ the emission angle, respectively.

Measurements and Data Evaluation

The flight speed of the aeroplane has again been held constant at about V_F = 60m/s. The test flights were directed both upwind and downwind. The flight height was h = 150 m. Two constant shaft speed settings n_1 = 2500 RPM and n_2 = 2600 RPM were employed. The recording of the sound signals began 500 m ahead of the flyover position and were stopped 500 m after microphone flyover. After each of the test flight series had been completed the azimuthal propeller/shaft-position was changed.

During flyover, the aeroplane was photographed in the overhead-position. Simultaneously the camera click was recorded on a separate channel of the multichannel tape recorder. With this impulse the relative position of the aeroplane and the sound impulses on the tape could be correlated.

The data evaluation of the sound signals received on the ground was performed with a 2-channel FFT-Analyzer both for time signatures and narrow band frequency spectra. The overhead position photographs were used to deterimine flight height and lateral deviation of the aeroplane for correction of the sound pressure.

Characteristic Pattern of the Sound Pressure Time-Histories

In order to determine the components of both the propeller and engine exhaust pressure, time-increments of 80 ms length

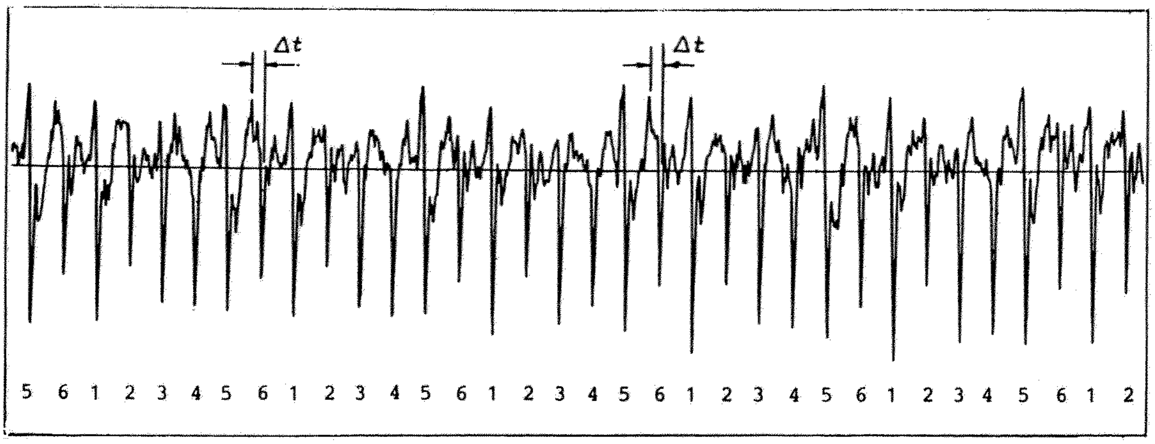

Fig. 15 Succession of Overall Sound Pressure Signals affected by Exhaust Contributions

were extracted. After identifying and numbering the individual noise impulses from the propeller and the engine exhaust, their development due to interference effects during the flight could be examined in detail.

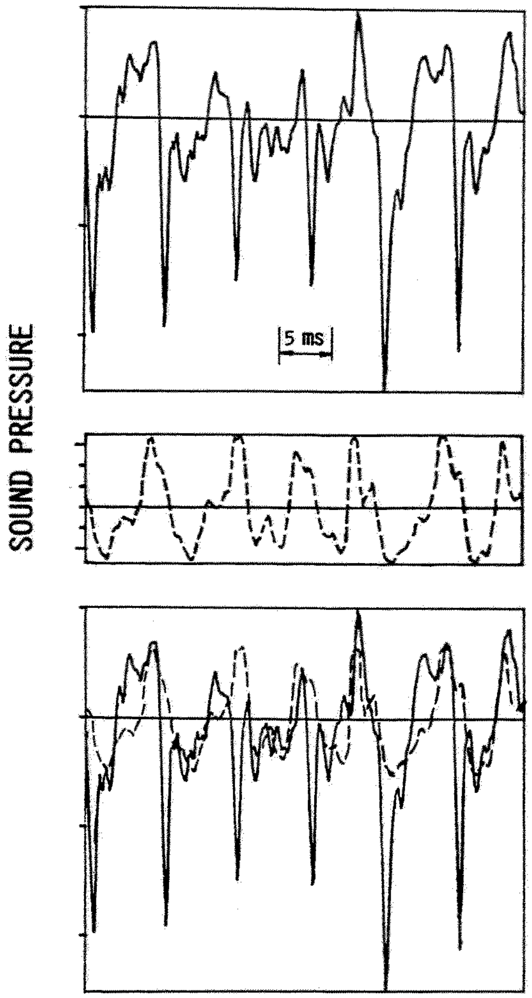

Fig. 16 Overall Sound Pressure Pattern (Top); Exhaust Sound Pressure Pattern (Centre). Overlapping of the Patterns illustrates the Interference Changes (Bottom).

Interference Process During Flight

The interference effects of overlapping sound pressures (attenuations and amplifications) measured in the near-field of the aeroplane had been shown in Fig. 13. A time sequence of sound pressure patterns as received by a ground microphone is shown in Fig. 15. This Figure displays impulses, which apparently are deformed in a "seemingly erratic" manner. A more detailed inspection of the patterns indicates however that every 6th impulse is affected in an individual way, such as being either attenuated or reinforced.

Presently it is supposed that these changes are due to engine exhaust noise. This appears likely because each of the 6 pulses of the engine noise is individually affected (see Fig. 5). Otherwise, a typical propeller noise pattern should consist of identically shaped pulses of equal spacing (see Fig. 8) as the propeller blades have the same shape and are equally spaced on the circumference of the propeller circle. The changes - certainly not being stochastic but rather corresponding to the working cycle of the 6-cylinder engine - cannot therefore be due to propeller irregularities. Fig. 16 shows a time sequence of the noise pressure pattern from a flyover for a shaft speed of n_2 = 2600 RPM (top of Figure). Overlapping this interference pattern and engine exhaust pattern clearly demonstrates that the observed changes are due to the engine exhaust noise. An engine exhaust noise pattern measured at the time of emission on board of the aeroplane at the same RPM (center of Figure) is superimposed upon the ground- measured noise pattern utilizing the individual characteristic features of the two traces. Using this method, the correct phase shift for adjusting the two pressure-time-histories now yields the final result, as shown on the bottom of the Figure. Now it becomes quite obvious which particular time delays of the patterns yield in-phase caused reinforcements and out-of-phase caused attenuations.

CONCLUDING REMARKS

It has been demonstrated that arranging the sound fields of a propeller and the piston engine exhaust in anti-phase seems indeed a viable technique to reduce the flyover noise of propeller aeroplanes equipped with piston engines. As the experimental results obtained in the near- and far-field of an aeroplane - a Cessna T 207 - in flight are very encouraging, the application of this noise reducing technique to a more suitable test aeroplane is presently prepared. Thus far reductions in sound pressure level of 4 to 6 dB(A) were obtained. Higher noise level reductions seem possible with optimizing the relative positions (especially their distance) of the sound sources of the aeroplane. The requirement for an improvement, particularly as phase shifting of the two sources is concerned, can be readily accomplished.

Ground stationary experiments with a Cessna 207 A test aeroplane are also in a preparatory stage. This aeroplane is emitting sequences of equidistant sound impulses from propeller and exhaust, allowing a much finder adjustment of the relative source patterns.

Symbols

a	Distance between Propeller plane and exhaust in m
B	Number of propeller blades
c	speed of the sound in m/s
c_f	Drag-thrust ratio
D	Propeller diameter in m
e	Distance of the exhaust to the propeller axis in m
F_n	Normalizing function
K_{nB}	Wave number related to the nB-order harmonics
m	Natural number designating the maxima
MH	Helical blade tip Mach-number
M_F	Flight Mach-number
n	Propeller speed in RPM; harmonic order
r	Ratio of reduction
t_A	Time span of the working cycle of the piston engine in ms
t_Z	Sequential time between two firings in ms
v	Airspeed in m/s
Z	Number of Cylinders of the piston engine
I'	Normalized intensity
ΔL_P	Noise level reduction
$\Delta\varphi$	Phase shift angle
$\Delta\varphi_{max}$	Largest aperture angle
ϑ	Emission angle
ϱ	Density
φ	Circumferential orientation in the propeller plane
φ_A	Circumferential orientation of the engine exhaust orifice
ϕ_A	Exhaust orifice velocity potential
ϕ_P	Propeller velocity potential
ϕ_R	Ratio of the velocity potentials
ω	Radian frequency in 1/s

Subscripts

e	Emission
F	Flight
M	Engine
P	Propeller
W	One shaft revolution
Z	Cylinder

References

|1| Lueg P., Verfahren zur Dämpfung von Schallschwingungen DRP Nr. 655 508. Anmeldetag: 27.1.1933. Erteilung: 30.12.1937.

|2| Nelson P.A., Curtis A.R.D., Elliot S.J., Quadratic Optimization Problems in the Active Control of Free and Enclosed Sound Fields. Proc. Inst. of Acoust., Spring Meet. York/U.K. 1985.

|3| Nelson P.A., Elliot S.J., The Minimum Power Output of a Pair of Free Field Monopole Sources. J. of Sound and Vibr. (1986) 105(1), 173-178.

|4| Ffowcs Williams J.E., Proceedings of the Royal Society of London, Series, A, 395, 63 - 88. Anti-Sound, 1984.

|5| Chaplin G.B.B., Chartered Mechanical Engineer 30, 41-47. Anti-noise - the Essex breakthrough, 1983.

|6| Bschorr O., Lärmminderung bei Propellertriebwerken, Offenlegungsschrift 2009105, 2. Sept. 1971.

|7| Kallergis M., Anordnung zur Minderung des Überfluggeräusches von Flugzeugen mit einem von einem Kolbenmotor getriebenen Propeller. Patentschrift DE 3735421. Erteilung 2.11.89.

|8| Kallergis, M., Minderung des Lärms von kolbenmotorgetriebenen Propellerflugzeugen durch gegenphasige Überlagerung der Drucksignale. Fortschritte der Akustik DAGA'88, S. 339-342

|9| Delfs, J., Überflugmessungen zur Ermittlung der gegen-/gleichphasigen Abstrahlung von Propeller- und Auspuffgeräuschen, DLR-IB 129-89/43, Nov. 1989.

|10| Kallergis, M., Möglichkeit einer aktiven Propellergeräusch-Dämpfung bei kolbenmotorgetriebenen Flugzeugen durch Änderung der Phasenbeziehung Propeller-/Motorauslaß. J. Acoustique 2 (1989) 401-406, Dez. 1989, P. 401 - 406.

|11| Goldstein M.E., Aeroacoustics, McGraw-Hill 1976.